Sensors & Actuators: A. Physical 351 (2023) 114174

Contents lists available at ScienceDirect

Sensors and Actuators: A. Physical

journal homepage: www.journals.elsevier.com/sensors-and-actuators-a-physical

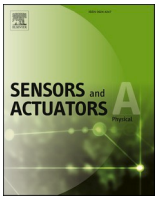

Study on ethanol driven by alternating current electroosmosis in microchannels

Yong Yu [a,*], Ji-Cheng Li [b], Hai Lin [a], Kai Li [a,c,**], Fu-ting Yi [d]

[a] CAS Key Laboratory of Microgravity, Institute of Mechanics, Chinese Academy of Sciences, Beijing 100190, China
[b] School of Energy and Power Engineering, Lanzhou University of Technology, Lanzhou 730050, China
[c] School of Engineering Science, University of Chinese Academy of Sciences, Beijing 100049, China
[d] Synchrotron Radiation Lab., Institute for High Energy Physics (IHEP), Chinese Academy of Sciences, Beijing 100084, China

ARTICLE INFO

Keywords:
Alternating current electroosmosis
Ethanol
Micropumps

ABSTRACT

Performance of alternating current electroosmosis (ACEO) in ethanol solutions containing three electrolytes, KOH, NH_4Cl and CH_3COONH_4, are investigated by using asymmetric microelectrode arrays and travelling-wave microelectrode arrays in microchannels. The experiment results show that for the ACEO flow induced by the asymmetric microelectrode arrays, only the flow in the ethanol solution containing KOH is stable and the most intensive, and the flow rate can be optimized with solution conductivity 20.2μS/cm and AC frequency range from 25 Hz to 125 Hz. For the case by the traveling-wave microelectrode arrays, only the ACEO flow in the ethanol solution containing CH_3COONH_4 is stable and the most intensive, and the flow rate can be optimized with solution conductivity 30.10 μS/cm in the ac frequency range from 10 Hz to 50 Hz. Moreover, no damage occurs on the microelectrodes after using of asymmetric microelectrodes and travelling-wave microelectrodes in the experiment.

1. Introduction

Microfluidics play an important role in many fields such as biology, chemistry, medicine, fluid science, electronics, materials science and mechanics [1–4]. Micropump technology is an essential tool to control small volume of fluid in microfluidic applications, so the research of micropump technology is of great significance [5,6]. Micropump technology has been studied in depth. Reviews on the micropump development are available in [7,8]. According to the working mechanism, micropumps can be divided into mechanical and non-mechanical ones. Mechanical micropumps contain moving parts, resulting in low reliability. It is hardly suitable for further miniaturized microfluidic devices. Non-mechanical micropumps have distinct advantages, such as high reliability due to no moving parts, and easy integration into microfluidic devices [9]. The fluids driven in microfluidic systems includes aqueous and non-aqueous ones. The aqueous solutions are widely used in the biological field, while non-aqueous solutions are widely used in micro fuel cells and electrical cooling systems [10–15].

Currently, the main non-mechanical micropumps that drive non-aqueous solutions in microfluidic systems are electrohydrodynamic (EHD) micropumps [15–30]. K. Aryana et al. reviewed EHD pumping and its achievements in heat transfer enhancement [23]. EHD pumps are classified into three categories: injection EHD pumps, conduction EHD pumps and induction EHD pumps. Injection EHD pumps work by using a high voltage electric field to inject free charges into a fluid through electrodes, thereby inducing flow [24]. The conduction pumps work by taking place an electrochemical reaction on the electrode surface to dissociate the solution molecules into ions. Ions drag adjacent liquids under the action of electric field to form a volume flow [25,26]. Travelling-wave induced electrohydrodynamic (EHD) is to establish the electrical property gradient of the fluid by the thermal gradient. Under the action of a three-phase traveling wave electric field, the ions are induced to move and drive the bulk flow [27–30]. The peak in velocity of traveling-wave EHD flows may be expected to occur when the traveling-wave frequency corresponds to the charge relaxation time ($f = 1/2\pi\tau$, with charge relaxation time constant $\tau = \varepsilon_r\varepsilon_0/\sigma$, relative permittivity ε_r, permittivity of vacuum ε_0 and electrical conductivity σ). But the actual peak in velocity occurs at a somewhat lower frequency than might be expected based on the charge relaxation time. [27].

Both injection EHD pumps and conduction EHD pumps require high

* Corresponding author.
** Corresponding author at: CAS Key Laboratory of Microgravity, Institute of Mechanics, Chinese Academy of Sciences, Beijing 100190, China.
E-mail addresses: yuyong@imech.ac.cn (Y. Yu), likai@imech.ac.cn (K. Li).

https://doi.org/10.1016/j.sna.2023.114174
Received 20 September 2022; Received in revised form 9 December 2022; Accepted 12 January 2023
Available online 13 January 2023

voltages to be applied to the electrode, at which the anode metal electrode generates cations. It will cause the electrode material to dissipate which seriously endangers the service life of the micropump. Therefore, how to prolong the working life of the working electrode of the EHD micropump is a key issue that is far from being resolved [29]. Moreover, the injection EHD pumps will degrade the electrical properties of the working liquid over time, and it is not appropriate for practical applications, and induction pump is not suitable for pumping an isothermal liquid due to need for heating [26]. But Traveling-wave induction EHD pumps has been proved effective for forced convective cooling of microelectronics benefiting from the anisotropic heating in the device environment [30].

The electroosmotic micropump, another promising non-mechanical micropump used in the microfluidic system, has been the focus of recent researches [31–33]. The application of direct current electroosmosis (DCEO) in microchannels has been studied theoretically and experimentally for a long time. In recent years, the study of alternating current electroosmosis (ACEO) has emerged [34–37]. The AC electroosmosis overcomes the shortcomings of DC electroosmosis, such as high voltage, easy electrolysis and easy bubble formation. Only a few voltages, mW power and mA current are needed to operate. Electrochemical reactions in the ACEO micropump are reduced or eliminated, thereby reducing the dissipation of the electrode material. These advantages make ACEO micropump has a broad application prospect in microfluidic system. The principle of AC electroosmosis is a capacitive charging mechanism. When the applied AC electric field is nonuniform, the normal component of the AC field to the electrode surface induces charge in the double layer, while the tangential component generates a body force on the induced charge, which drives the liquid to move [38]. According to the microelectrode arrangement, AC electroosmotic micropumps are divided into three types [39]: micropumps with asymmetric co-planar electrodes (AM), micropumps with 3D or non-planar electrodes (3DM) and traveling-wave electroosmotic micropumps (TWM). The traveling-wave electroosmotic micropump employs a traveling wave signal similar to the induction EHD pump. However, the former three electrokinetic pumps, including injection EHD, conduction EHD, and induction EHD, are originated by electrostatic forces in the bulk fluid phase, while electroosmosis (including DCEO and ACEO) arises from the electrostatic forces within the thin electrical double layer. In the application of traveling wave electroosmosis, ions in the double electric layer are subjected by tangential electrical forces along the direction of the traveling wave, thus driving the volume flow [40]. Therefore travelling-wave electroosmosis micropump do not require heaters to generate temperature differences in the microchannel.

So far, the research on ACEO flow has been carried out for more than 20 years, but in the field of electroosmosis, the research on DCEO is still the majority, and there are few reviews on the whole field of electroosmosis [32,33]. However, a lot of important research work has been carried out in the research of ACEO flow, mainly in the asymmetric electrode micropumps [36–37, 41–45], 3D electrode micropumps [46–50], traveling-wave electroosmotic micropumps [38 , 51–53], and dc bias micropumps [31,54,55]. A series of new type of ac electroosmotic micro-pump were further developed, for example, Sugioka et al. [43] developed a ratchet ACEO pump containing both ratchet and plane electrodes. Yoshida et al. [44] presented a novel AC electroosmotic micropump using a square pole – slit electrode array called the SS-ACEO-MP. Guo et al. [50] described for the first time a 3D stepped microelectrode array on a flexible Kapton substrate. Weiyu Liu et al. [56, 57] realized localized trapping and concentration of nanoparticles in a continuous bulk electroosmotic flow driven by a DC-biased AC voltage signal. However, there is still no obvious breakthrough in the theoretical difficulties of AC electroosmosis, such as the theoretical explanation of flow direction reversal phenomenon in AC electroosmosis under high voltage and high frequency conditions. In addition, the current research on ACEO micropump technology mainly focuses on aqueous solution, while the non-aqueous ACEO driving technology has not been studied.

Ethanol or ethanol aqueous solution can be used as an excellent refrigerant and is also a typical renewable, green and environmentally friendly energy source [58]. Moreover, direct ethanol fuel cells are an important trend in fuel cell [59]. However, studies on the AC electroosmosis drive of ethanol are still lacking. Xie et al. [60] claimed to carry out the experiment and simulation on driving ethanol by using the traveling-wave electroosmotic micropump. Actually, no electrolyte was injected into the ethyl ethanol in the experiment. Although electroosmotic flow occurs at low ion concentration, the ion concentration in pure ethanol is too low to induce AC electroosmotic flow, requiring the addition amount of trace electrolyte. Just like in an aqueous solution for AC electroosmotic drive, a small amount of KCl is added to pure water to improve the conductivity. Therefore, ions could only be generated from the anode metal or by electrochemical reactions in the ethanol solution, which is the EHD pumping mechanism. In the application of AC electroosmosis, the electric field mainly affects the ions in the double electric layer to drive the volume flow, so the addition of different electrolytes has a great influence on ACEO flow. Different ions have different charges, different volumes, and different mobility, so the AC electroosmosis will be different. In this paper, the asymmetric microelectrode array and traveling wave microelectrode array were used, and different electrolytes were added to the ethanol solution for the first time to investigate the ACEO flow experiment. The results show that ethanol solution with different electrolytes has significant influence on the performance of ACEO micropumps. After optimizing the electrolyte concentration and experimental conditions, the voltage required to drive the ethanol solution is significantly reduced, and the electrode is not damaged, which is better than the EHD method.

2. Experimental equipment and methods

2.1. Design of asymmetric and traveling-wave microelectrode arrays

The ACEO flow in microchannel induced by interdigitated asymmetric gold electrodes arrays plated on glass substrates is studied to investigate the actual pumping effects. According to our previous study on aqueous solutions [42], the optimal geometry of the single pair of asymmetric electrodes has a width of 100/10 μm and a gap 20 μm (see Fig. 1 A). The asymmetric microelectrode arrays, each consisting of three identical pairs of asymmetric electrodes, are shown in Fig. 1B-1D. The interval between the electrode pairs is 50 μm, 100 μm and 150 μm respectively.

Fig. 2 shows the manufacturing process of the travelling-wave microelectrode array chip. As shown in Fig. 2 A, the first step is to coat the quartz glass substrate with photoresist and then expose the electrode structure to obtain the photoresist structure. The next step is to coat the entire surface with chrome-gold metal layer by vacuum evaporation technique and then remove the photoresist and the metal layer on the surface of the photoresist to obtain the structure of the metal electrode. Fig. 2B shows the 1 and 2 quadrant metal electrode structures obtained by the above process. Fig. 2 C shows the insulating isolation structure made of negative SU8 photoresist. It requires the use of the carved technique to lithograph the insulating structure exactly to the position where the 1 and 2 electrodes need to be insulated. Fig. 2D shows the 3 and 4 quadrant electrodes structure produced by the stripping process of process A and the carved technique C. The 3 and 4 quadrant electrode structures cross the lead wire of 1 and 2 quadrant electrode structures through the insulation structure as shown in Fig. 2 C to realize the separation of the lead wire of 4 quadrant electrodes and complete the production of the whole electrode structure. Two travelling-wave ACEO microelectrode arrays, with electrode widths and intervals of 10 and 20 μm, are shown in Figs. 2E and 2 F. The Polydimethylsiloxane (PDMS) microchannel has a length of 5 cm, a width of 800 μm and a depth of 500 μm. The microchannel is sealed on the electrode, and the length direction of the microchannel is perpendicular to the length direction of

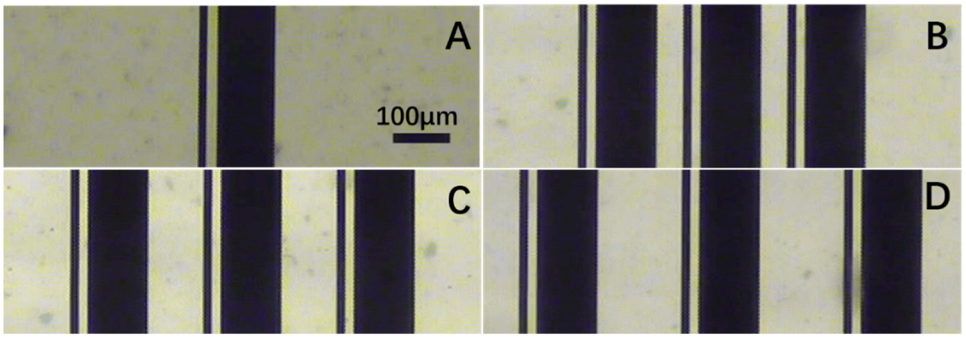

Fig. 1. (A) A single pair of interdigitated asymmetric gold electrodes with the geometry of 100/10 μm in width and with 20 μm gap. Asymmetric microelectrode arrays consisting of three identical asymmetric electrodes pairs with the interval designed as (B) 50 μm, (C) 100 μm and (D) 150 μm respectively.

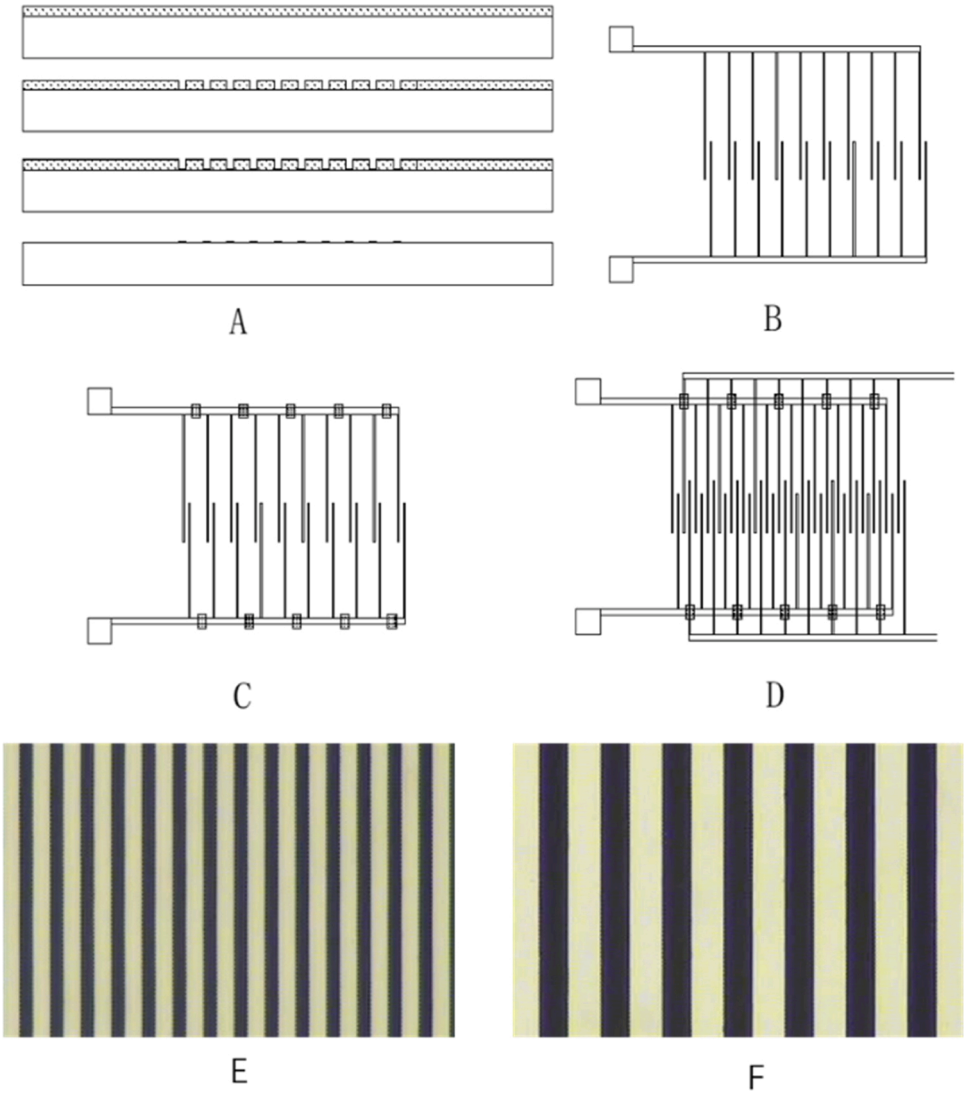

Fig. 2. (A)-(D) Microelectrode processing process flow chart and the travelling-wave ACEO microelectrode array. Travelling-wave ACEO microelectrode arrays with electrode widths and intervals of (E) 10 μm and (F) 20 μm.

the microelectrode. Two cylindrical ports of 2 mm in diameter are created using a puncher in the PDMS microchannel to serve as an exit and entrance. Two silica gel pipes with an outer diameter of 2 mm and an inner diameter of 0.5 mm and a length of 10 cm were inserted at the outlet and entrance of the microchannel. Since ethanol is volatile, the connection between the tube and the microchannel needs to be sealed with Silicone Rubber. After the solution was injected into the microchannel, the outer mouth of the two silica gel tubes was connected through a stainless steel pipe with an outer diameter of 0.7 mm, an inner diameter of 0.51 mm and a length of 10 mm to form a sealed loop.

2.2. Experimental equipment

A signal generator (TGA1244, TTI, UK) is used to generate a sinusoidal AC voltage signal to power the electrodes to induce the AC electro-osmotic flow in the microchannel. The voltage values used in the experiment is the peak-to-peak voltage values. The fluid flow is observed by a microscopy (XSP-22AY, Shanghai Optical Instrument Factory, China) vertical to the glass substrate and recorded by a charge coupled device (CCD) (Mintron Company, China) and a video capture card (MP400s, Gaochuang Company, China). The CCD used in the experiments is 25 frames per second and the oscilloscope is a DS4014 (DS4014, RIGOL company, China). Electrochemical measurements are performed on CHI 1230 electrochemical workstation (CHI 1230, Shanghai Chenhua company, China).

2.3. Experimental methods

2.3.1. Electrolytes

The electrical conductivity of the solution can be expressed as:

$$\sigma = F\sum_i |Z_i| u_i C_i \quad (1)$$

Where σ is the electrical conductivity, F is Faraday's constant, $|Z_i|$ is charge number carried by charged body, C_i is the molar concentration of a charged substance and u_i is the mobility of the charged body. Mobility can be calculated by Eq. (2).

$$u_i = \frac{e|Z_i|}{6\pi r}\frac{1}{\eta} \quad (2)$$

Where η is viscosity, and r is the radius of the charged body. It can be seen that the conductivity of the solution is inversely proportional to the dynamic viscosity of the working medium. Therefore, at the same electrolyte concentration, ethanol has a lower electrical conductivity than water due to its greater viscosity.

Three electrolytes soluble in ethanol are studied, i.e. potassium hydroxide (KOH), ammonium chloride (NH_4Cl) and ammonium acetate (CH_3COONH_4). Solid KOH was dissolved in water, and then KOH solution is injected into ethanol to obtain a concentrated electrolyte solution with a concentration of 0.2 mol/L. The solvent for the concentrated electrolyte solution contains 80% ethanol and 20% water. NH_4Cl and CH_3COONH_4 are directly dissolved in pure ethanol to obtain concentrated electrolyte solutions with concentrations of 0.2 mol /L and 0.5 mol /L.

2.3.2. The measurement of AECO flow rates

The concentrated electrolyte solutions are injected into ethanol, and the fluid conductivity is measured by a conductivity meter (DDSJ-308 F, Shanghai Electric Instrument Co., Ltd.). The polystyrene pellets (Tianjin BaseLine ChromTech Research Centre) with the diameter of 1 μm are seeded to trace the microflow. The solution of polystyrene particles was precipitated by centrifugation. Removing the solution, the centrifuged polystyrene particles are dispersed in ethanol. The motion of flow tracers is recorded on video, and then converted to images. Then the flow rate can be calculated by tracking the tracer motion. The motion of the tracers in the vicinity of the electrodes is tracked, and the average particle velocity is calculated. The uncertainty is given by the dispersion of the particles. The flow field is obtained by the particle image velocimetry software (Microvec Pte. Ltd., Beijing, China).

The 1 μm PS particle is considered to suffer from a non-negligible DEP force field adjacent to the electrode array where the electric field attains a maximum at electrode rims. So, the total moving velocity of tracer particles in effect a linear combination of fluid flow due to ACEO and electrokinetic motion in a field gradient due to DEP. Seungkyung Park et al. [61] studied the Alternating current (ac) electrokinetic motion of colloidal particles suspended in aqueous medium and subjected to a spatially nonuniform ac electric field, analyzed the relative magnitudes of dielectric electrophoresis, electrophoresis, AC electroosmosis and Brownian motion. It is considered that polystyrene pellets are mainly affected by alternating current electroosmosis in microsystems with low conductivity, low voltage and low frequency. The tracer particles of the polystyrene pellets used in the experiment are neutral particles with little charge. Therefore, under the condition of low voltage and low frequency AC electric field, there will be no obvious electrophoresis effect if the charge of particles is small.

2.3.3. The electrochemical measurements

Three-electrode system is adopted for electrochemical measurement. Gold disk electrode (diameter 0.5 mm, area 0.196 mm^2) is the working electrode, AgCl/Ag (KCl sat) is the reference electrode, and the counter electrode is titanium chip electrode. Reference electrodes are all configured with Luggin capillary. The temperature in the experiment is 298 K, the room temperature.

3. Results and discussion

3.1. The ACEO flow induced by the asymmetric microelectrode arrays

The experiments are performed on ethanol solutions with three electrolytes using the single asymmetric microelectrode pair as shown in Fig. 1 A. To measure the flow velocity within the range of 30 μm to the left edge of the narrow electrode, 20 random particles are selected. Fig. 3 shows the averaged horizontal velocity of ACEO flow induced by the single pair of asymmetric electrodes. Take the direction from the small electrode to the large one as the positive direction. It can be seen that for the ethanol solution containing CH_3COONH_4, the ACEO flow only occurs in a narrow frequency range less than 10 Hz with negative flow rates. For the ethanol solution containing NH_4Cl, the ACEO flow occurs in the frequency range up to 70 Hz. However, the flow is relatively weak and the flow direction reverses at about 2 Hz. For the ethanol solution containing KOH, the ACEO flow is stable from the narrow electrode to the wide one in a much wider frequency range. The flow rates are intensive in a frequency range from 10 Hz to 60 Hz. Note that for the aqueous solutions, the ACEO flow also reverses the flow direction under high voltage and high frequency [60]. However, for the ACEO flow in the ethanol solutions containing NH_4Cl and CH_3COONH_4, the flow reverses its direction under low voltage and low frequency. It indicates the significant influence of the ion types on the characteristics of ACEO flows.

Then experiments are performed on the ethanol solutions containing KOH by using the asymmetric electrode array with the interval 100 μm (shown in Fig·1 C) . Fig. 4 shows the influence of solution conductivity on the ACEO flow rates. It can be seen that the most intensive ACEO flow rate occurs at a solution conductivity of 20.2μS/cm. Fig. 5 shows the influence of the interval between the microelectrode pairs on the ACEO flow rates. The profiles are nearly in the same trend, however, the ACEO flow can be optimized by the interval 100 μm between the electrode pairs to exhibit the most intensive flow rates and the widest operation frequency range, which is also due to electric field interference between electrode pairs.

Since the flow rate of ACEO is proportional to the square of the applied AC voltage, experiments are performed on the effect of applied AC voltage on the flow rates to verify the mechanism which the flow occurs. The experimental results in Fig. 6 show that the flow rate first increases with the increase of applied AC voltage, reaching a maximum value at 6.5 V, and then decreases with the increase of applied AC voltage. When the applied AC voltage is less than 6 V, the flow rate is linear with the square of the applied AC voltage. Therefore, solution flow is considered to be caused by ACEO when the applied AC voltage is less than 6 V.

The results show that the ethanol solution can be driven by using asymmetric microelectrode arrays and low voltage after the optimal

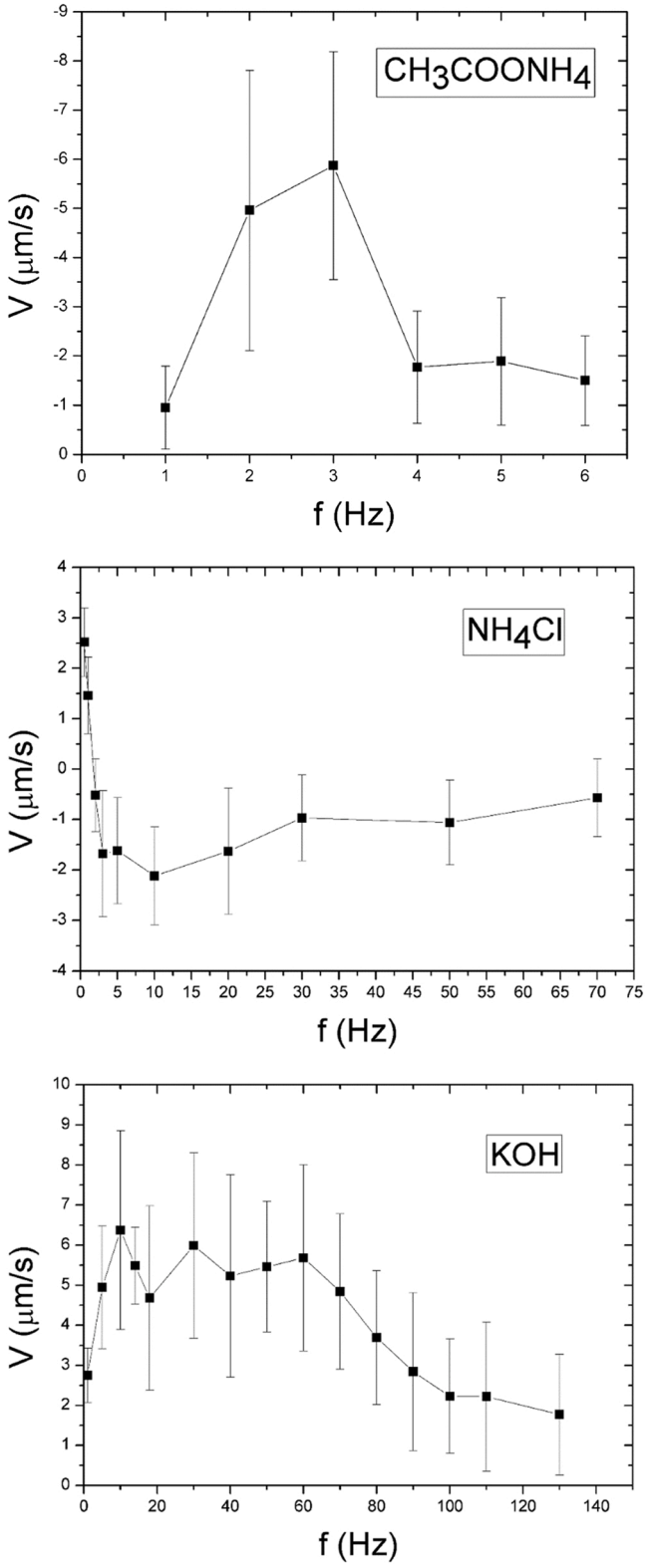

Fig. 3. Averaged ACEO flow rate induced by the single pair of asymmetric electrodes in the vicinity of 30 μm to the left edge of the narrow electrode in ethanol solutions containing NH_4Cl, CH_3COONH_4 and KOH respectively. The applied AC voltage is 5 V; 25 ℃; the geometry of the single pair of asymmetric electrodes is 100/10 μm in width with 20 μm gap; the conductivity is 30.4μS/cm; the fluid is observed through a microscope focused at 9.6 μm above the electrode.

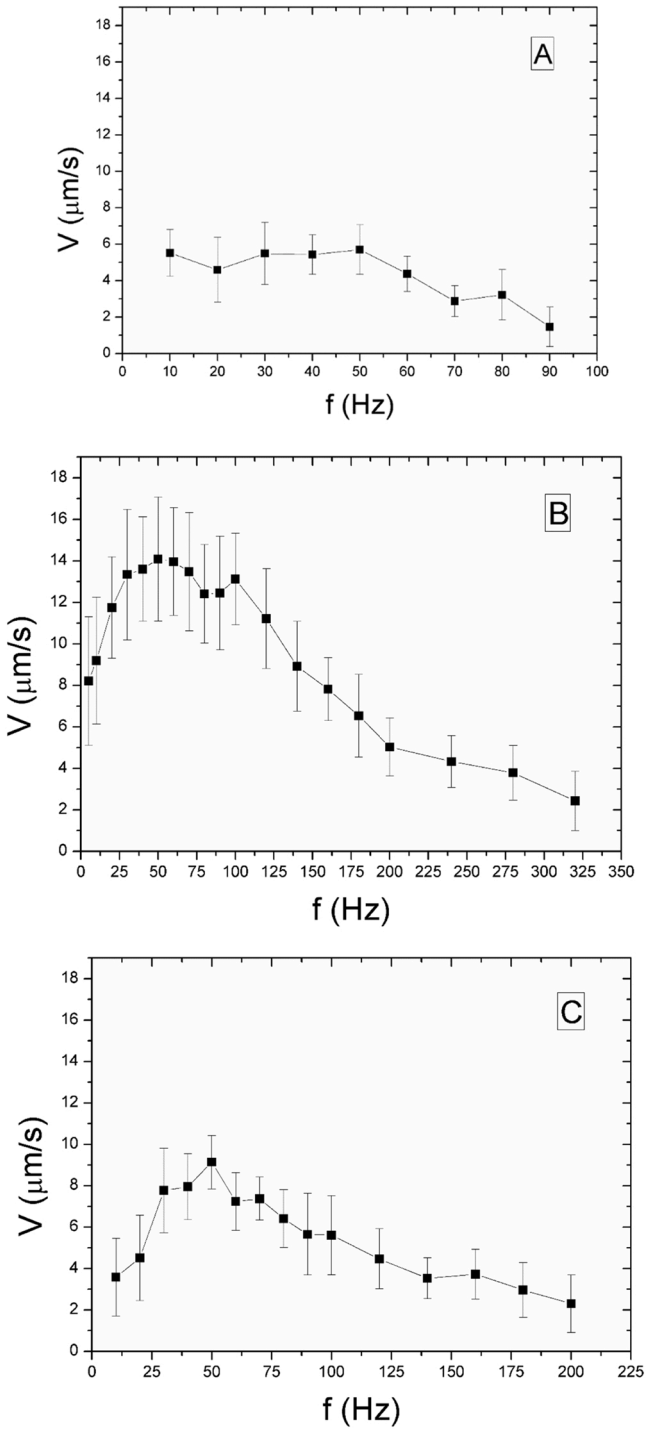

Fig. 4. Influence of conductivity of ethanol solution containing KOH on the ACEO flow rates using asymmetric microelectrode arrays. The applied AC voltage is 5 V; 25 ℃; the fluid is observed through a microscope, focused at 9.6 μm above the electrode; the gap between the asymmetric electrode pairs was 100 μm; the conductivity is: (A) 10.03 μS/cm, (B) 20.02 μS/cm and (C) 30.03 μS/cm.

electrolyte is added to the ethanol solution. The microelectrode arrays can be used in ethanol solution containing electrolyte for a long time, and no microelectrode damage was observed. This method shows better performance than EHD method.

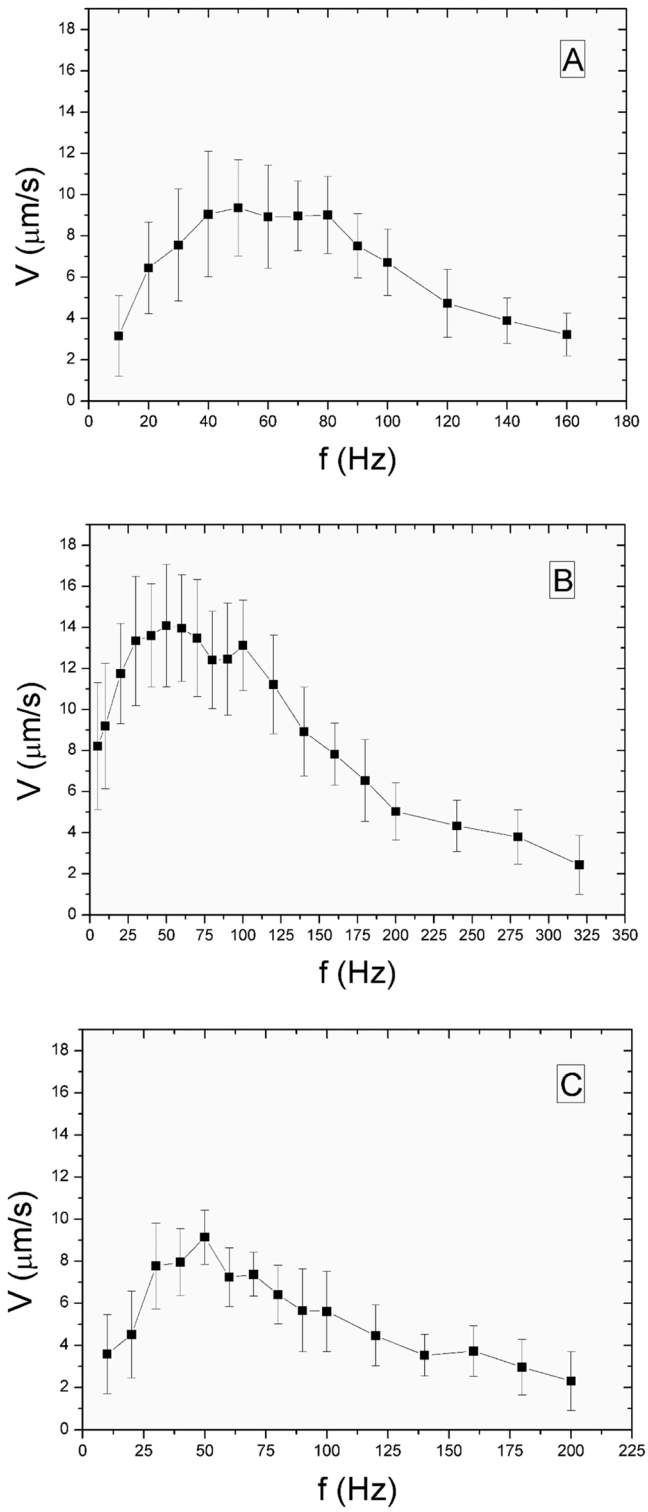

Fig. 5. Influence of the interval between the asymmetric microelectrode pairs on the ACEO flow rates in ethanol solution containing KOH. The applied AC voltage is 5 V; 25 ℃; the fluid is observed through a microscope, focused at 9.6 μm above the electrode; the conductivity is 20.02 μS/cm; the gap between the asymmetric electrode pairs is : (A) 50 μm, (B) 100 μm and (C) 150 μm.

3.2. The ACEO flow induced by the traveling-wave microelectrode arrays

The ACEO flow in ethanol solutions containing KOH, NH_4Cl, and CH_3COONH_4 by using the traveling-wave microelectrode arrays are also investigated. As shown in Fig. 2, the alternating current of the same frequency and voltage is applied to the four quadrant electrodes, but with different phase angles of 0°, 90°, 180°, 270° respectively. As shown in Fig. 7, the ACEO flow in the ethanol solutions containing KOH or NH_4Cl is disordered. While the ACEO flow in the ethanol solution containing CH_3COONH_4 is stable, as shown in Fig. 8. The flow rate in the ethanol solution containing CH_3COONH_4, is the most intensive and nearly remains constant in the frequency range from 10 Hz to 50 Hz, with a solution conductivity of 30.10 μS/cm. Fig. 9 shows the influence of the electrode width and the interval between the microelectrode pairs on the flow rate in the ethanol solution containing CH_3COONH_4. The results show that the flow rate increases with the decrease of the electrode width and interval of microelectrode pairs. Similar to the asymmetric microelectrode arrays, no damage to the microelectrodes is found after reusing the travelling-wave microelectrode arrays. Furthermore, the actual operation voltage for driving the solution flow is only around 4 V, which is much lower than that used in the EHD method.

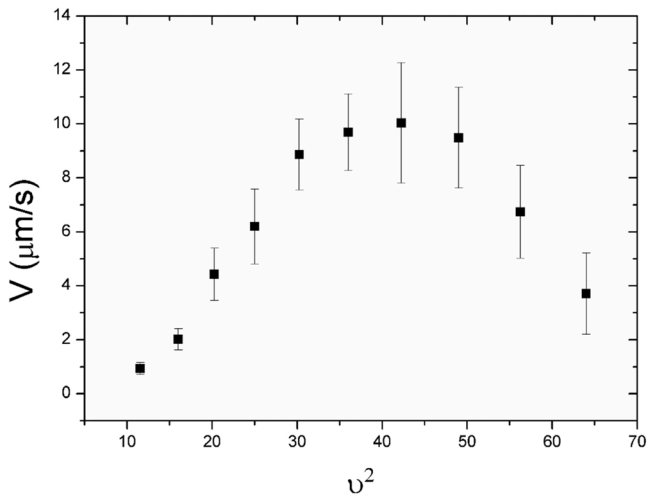

Fig. 6. Influence of the square of the applied AC voltage between single pair of asymmetric electrodes on the ACEO flow rates in ethanol solution containing KOH. The geometry of the single pair of asymmetric electrodes is 100/10 μm width with 20 μm gap; the frequency f is: 50 Hz; The temperature is 25 ℃; the conductivity is 20.01 μS/cm; the fluid is observed through a microscope focused at 9.6 μm above the electrode.

Experiments on the effect of applied AC voltage on the flow rates are also carried out to verify the mechanism by which the flow occurs. As shown in Fig. 10, with the increase of the applied AC voltage, the flow rate first increases gradually, reaching its maximum value at 5.5 V, and then decreases with the increase of the applied AC voltage. When the applied AC voltage is less than 5.5 V, the flow rates also linear with the square of the applied AC voltage. Therefore, the solution flow is considered to be caused by ACEO when the applied AC voltage is less than 5.5 V. Thus, the ACEO drive of ethanol solution can be achieved by adding an optimized electrolyte to the ethanol solution and applying a low voltage to the traveling-wave microelectrodes array.

3.3. The electrochemical measurements

The experiments results showed that the ion type has a significant effect on the flow of ACEO. To investigate the mechanism, electrochemical experiments are carried out to investigate the electrochemical reactions on the electrode surface to evaluate the effect of Faraday current.

Tremiliosi-Filho et al. [63] studied the electrochemical behavior of ethanol on the gold electrode in dilute alkaline aqueous solutions. They found the oxidation reaction of ethanol is complex, and the oxidation products depends on the properties of the liquid. In the present study, electrochemical measurements are conducted on the ethanol solutions

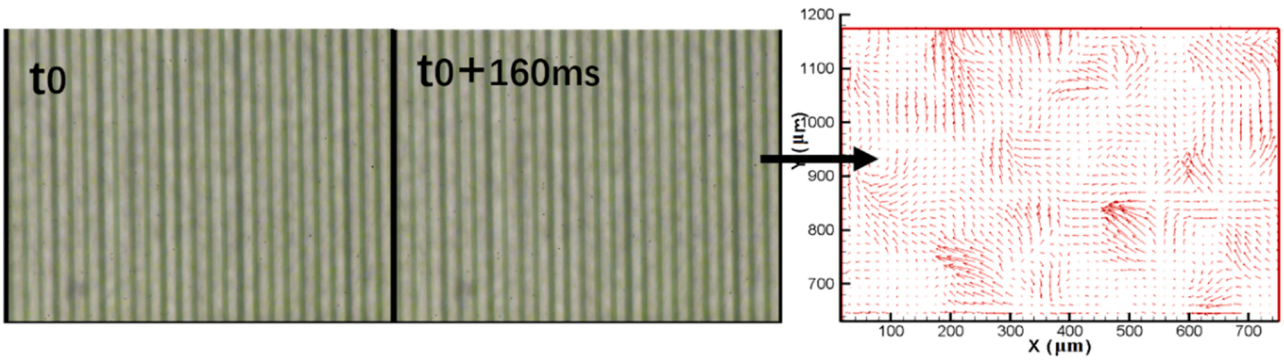

Fig. 7. Bird's eye view of the ACEO flow of the ethanol solution containing NH_4Cl induced by the traveling-wave microelectrode arrays. The applied voltage and frequency are 4 V and 10 Hz at 25 ℃; the fluid is observed through a microscope, focused at 19.2 μm above the electrode; the electrode width and interval of the travelling-wave microelectrode array are both 10 μm; the conductivity is 30.4μS/cm.

containing different electrolytes on gold electrode by cyclic voltammetry.

Fig. 11 shows the cyclic voltammetry of ethanol solutions containing different electrolytes at a gold electrode. Figs. 12–14 show the profiles of the REDOX current in ethanol solutions containing different electrolytes at different solution conductivities. For the solution containing KOH, local anodic peaks at 0.46 V and 1.28 V vs. Ag/AgCl are observed for all the cases studied. On the other hand, local cathodic peak is observed at − 1.74 V and − 1.52 V vs. Ag/AgCl respectively in the solution with the conductivity of 30.3μS/cm and 40.2μS/cm, but no cathodic peak is observed in the solution with the conductivity of 20.3μS/cm. In consideration of the current density, the cathode reaction is more significant than the anode reaction. The anodic peak current increases with the conductivity (hydroxide ion and pH value), but the corresponding potential is nearly constant. It indicates that the anodic peaks correspond to the oxidation of ethanol on the gold surface. In an alkaline solution, ethanol is primarily oxidized with acetic acid [63]. The anode reaction is $CH_3CH_2OH \rightarrow CH_3COO^- + H^+ + e$ and the cathode reaction is $2C_2H_5OH + 2e \rightarrow 2C_2H_5O^- + H_2$.

For the solution containing NH_4Cl, only a weak local anodic peak is observed at 1.18 V vs. Ag/AgCl. In the potential range larger than 1.3 V, the oxidation current increases quickly, indicating the rapid oxidization of the ethanol on the gold surface. During the reverse scan, a weak peak is observed at 0.86 V while two significant cathodic peaks are observed at 0.34 V and − 0.75 V. The cathode reaction is similar to the anode reaction in terms of current density, and the cathode reaction is slightly intensive than the anode reaction. With the increase of the electrical conductivity, the REDOX current increases while the corresponding cathode potential is nearly constant. The ethanol solution containing NH_4Cl is slightly acidic, and the main oxidation product is acetaldehyde (CH_3CHO) with a small amount of acetic acid (CH_3COOH) [63]. The anode reaction is $CH_3CH_2OH \rightarrow CH_3CHO + H^+ + e$ or $2Cl^- \rightarrow Cl_2 + e$, and the cathode reaction is $2C_2H_5OH + 2e \rightarrow 2C_2H_5O^- + H_2$ or $2NH_4^+ + 2e \rightarrow H_2 + 2NH_3$.

Using NH_4Cl as the electrolyte, electrochemical reactions do produce a portion of the gas. Combined with the experimental results in Fig. 7, it could be considered that the gas generated by electrochemical reaction interferes with the flow when traveling wave electrode array are used.

For the solution containing CH_3COONH_4, two weak local anodic peaks are observed at 0 V and 0.42 V vs. Ag/AgCl, and one significant anodic peak is observed at 1.47 V vs. Ag/AgCl. During reverse scan, there are significant cathode peaks at 0.20 V and − 0.88 V vs. Ag/AgCl. The cathode reaction is also more intensive than the anode reaction. With the increase of electrical conductivity, the REDOX current increases. The corresponding anodic potential increases, while the corresponding cathode potential is nearly constant. The ethanol solution containing CH_3COONH_4 is nearly neutral, and the main REDOX reaction is similar to ethanol solution containing NH_4Cl [63]. However no gas interference was found in the flow. So the anode reaction is $CH_3CH_2OH \rightarrow CH_3CHO + H^+ + e$ and the cathode reaction is $2C_2H_5OH + 2e \rightarrow 2C_2H_5O^- + H_2$.

As shown in Fig. 11, the electrochemical reaction will occur on the surface of the gold electrode at low voltage. Among the three electrolytes, the REDOX currents in the ethanol solution containing KOH is the most intensive, while the REDOX currents of ethanol solution containing CH_3COONH_4 is the lowest. According to the electrochemical reactions analyzed above, the main components participating in the electrochemical reactions come from the solution rather than the microelectrode dissipation. The voltages applied in the experiment were also low, so the electrodes were not damaged.

In the experiments of the ACEO flow in aqueous solutions, the flow direction reverses under high voltage and high frequency [52 , 62, 64]. A possible explanation for the flow reversal in asymmetric microelectrode arrays may be attributed to the steric effects in capacitive charging. High voltage induction across the double layer leads to the ion aggregation and the decrease in surface capacitance [62,64,65], i.e. the steric effects. The flow reversal phenomenon of the traveling-wave microelectrode arrays is considered to have a different physical origin from that of asymmetric microelectrode arrays [54]. It is considered that the countercurrent phenomenon of travelling wave microelectrode array may be caused by Faraday reaction [64 , 66–68]. The Faradaic reactions generates ionic concentration gradient in the bulk solution, resulting in electrolyte conductivity gradient. The conductivity gradient causes a surface flow in the opposite direction [67]. Different migration rates of positive and negative ions may also play a role [64]. González et al. [31,68] theoretically studied the combined effects of Faradaic reactions and ion mobility differences on the ACEO flow and predicted reversed flow in travelling-wave electroosmosis. The flow inversion for asymmetric arrays may have a different physical origin from that for traveling wave systems, but it is also possible that both Faraday mechanism and steric effect exist simultaneously. However, because the size of asymmetric electrode is much larger than that of travelling-wave electrode, steric effect should be greater in asymmetric electrode arrangements.

Among the three electrolytes, the REDOX currents in the ethanol solution containing KOH is the most intensive, while the REDOX currents of ethanol solution containing CH_3COONH_4 is the lowest. This may explain why the ethanol solution containing CH_3COONH_4 has a better ACEO flow, using the traveling-wave microelectrodes arrays. The migration rate of K^+ should be greater than that of NH_4^+, and the migration rates of OH^- and Cl^- should also be greater than that of CH_3COO^-, and NH_4^+ and CH_3COO^- have larger volumes. So CH_3COONH_4 electrolyte is more prone to steric effects. Compared with NH_4Cl and CH_3COONH_4 electrolytes, KOH electrolyte is less prone to steric effect. This may explain why the ethanol solution containing KOH has a better ACEO flow, using the asymmetric microelectrode arrays. For

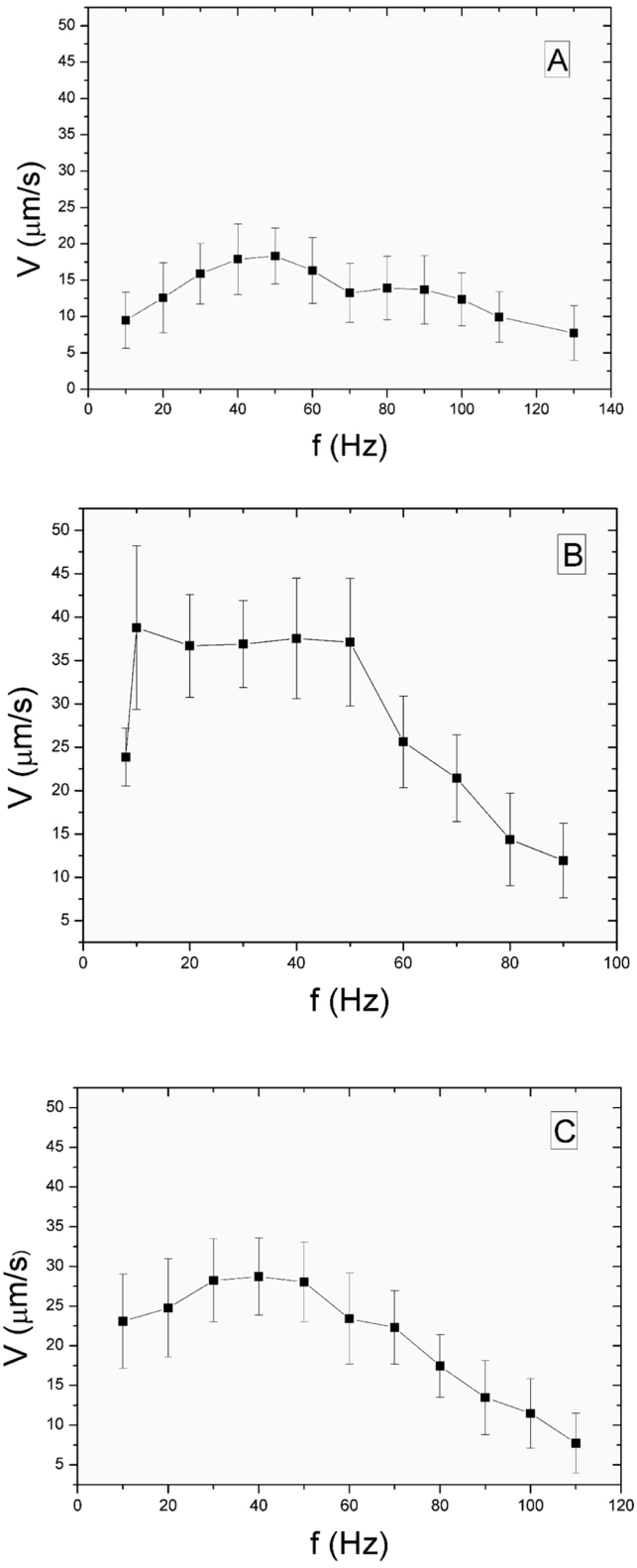

Fig. 8. Influence of conductivity of ethanol solution containing CH_3COONH_4 on the ACEO flow rate using the traveling-wave microelectrodes array. The applied AC voltage is 4 V at 25 ℃. The fluid is observed through a microscope, focused at 9.6 μm above the electrode; the electrode width and the interval between the microelectrode pairs is 10 μm, as shown in Fig. 2 (E). The flow conductivity is : (A) 20.10 μs/cm, (B) 30.10 μs/cm and (C) 40.00 μs/cm respectively.

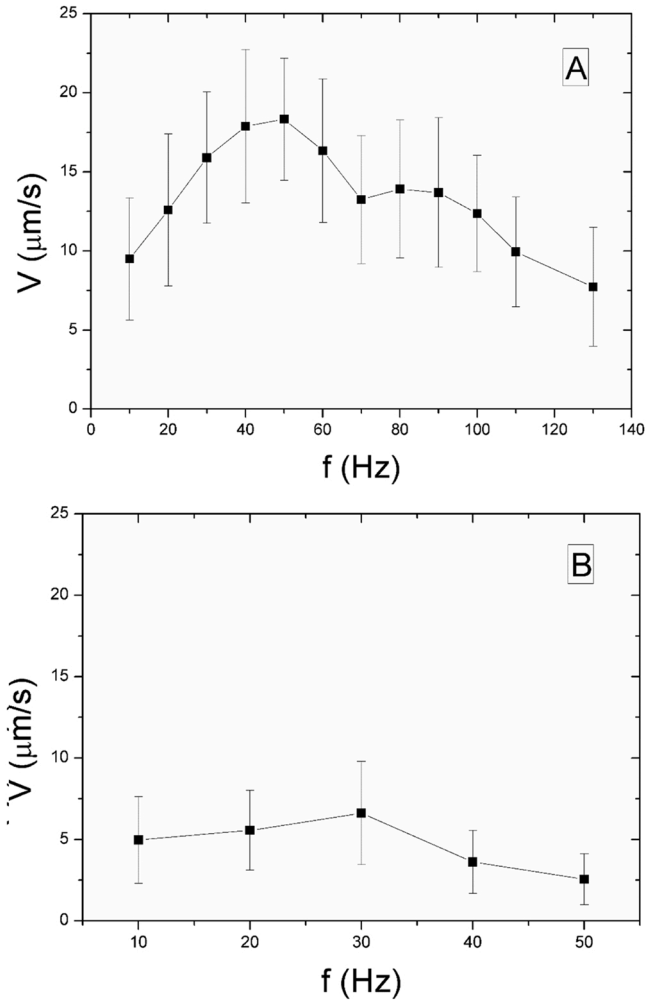

Fig. 9. Influence of the electrode width and interval of the traveling-wave microelectrodes array on the flow rates in ethanol solution containing CH_3COONH_4. The applied AC voltage is 4 V at 25 ℃; the fluid is observed through a microscope, focused at 9.6 μm above the electrode; the conductivity is 20.10 μS/cm, and the electrode width and interval between the microelectrode pairs is: (A) 10 μm and (B) 20 μm respectively.

the solution containing NH_4Cl, both anodic and cathodic reactions produce gas. The gas produced by Faraday reaction may be responsible for the disordered flow in the ethanol solutions containing NH4Cl in the traveling-wave ACEO experiments.

The current experimental results showed that the traveling-wave electrode arrays is more likely to be affected by Faraday current in AC electroosmosis, while the asymmetrical electrode arrays is more likely to be affected by steric hindrance. However, the electrochemical reaction of ethanol solution is very complicated, and the study of the electric double layer on the electrode surface is always difficult. Therefore, this problem needs further study and the existence of unknown mechanisms cannot be ruled out. It may be necessary to look for some special experimental methods in order to investigate this problem further. If a new theoretical explanation can be proposed, the simulation method may also solve this problem.

4. Conclusion

The performance of ACEO of ethanol solutions containing electrolytes KOH, NH_4Cl and CH_3COONH_4, are investigated by using asymmetric microelectrode arrays and travelling-wave microelectrode arrays.

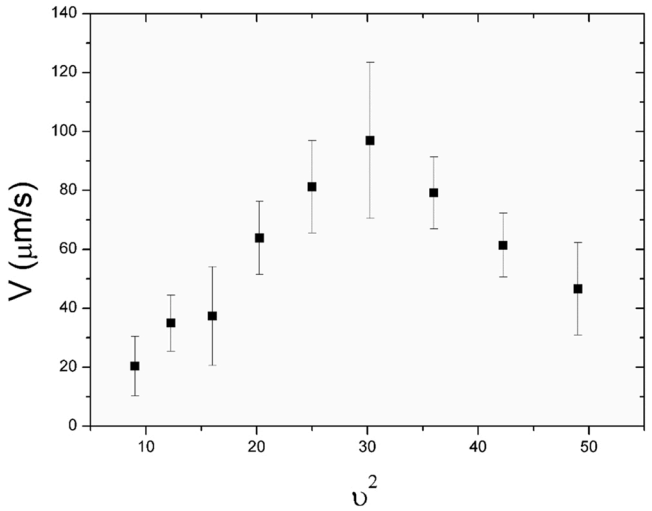

Fig. 10. Influence of the square of the applied AC voltage on the ACEO flow rates in ethanol solution containing CH_3COONH_4 using the traveling-wave microelectrodes arrays at 25 ℃. The electrode width and the interval between the microelectrode pairs is 10 μm as shown in Fig. 2 (E). The fluid is observed through a microscope, focused at 9.6 μm above the electrode; the flow conductivity is 30.10 μs/cm and the frequency f is 40 Hz.

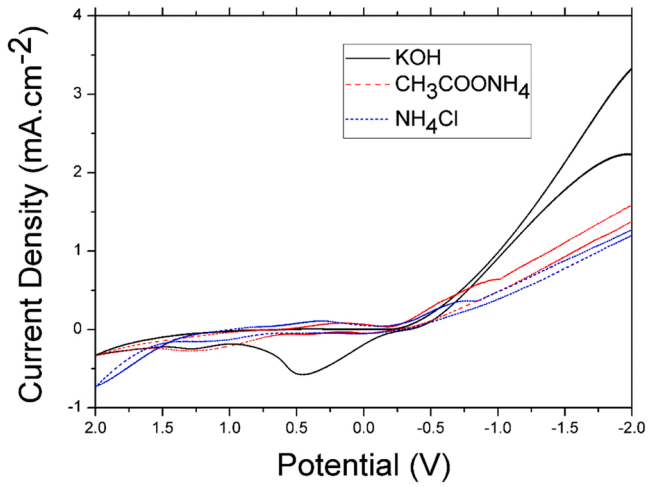

Fig. 11. Cyclic voltammograms of ethanol solutions containing different electrolytes on gold electrode. Scanning rate: 100 mV/s. Scaning from − 2–2 V, and sweeping back to − 2 V after reaching 2 V. Ag/AgCl. The conductivity is 20.03μS/cm.

For asymmetric microelectrode arrays, only the flow in the ethanol solution containing KOH is stable and most intensive. It is considered that the solution flow is caused by ACEO when the applied AC voltage is less than 6 V. In the parameter range studied, the flow rate is optimized with the interval between the microelectrode pairs 100 μm, the solution conductivity 20.2μS/cm and ac frequency range from 25 Hz to 125 Hz.

For traveling-wave microelectrode arrays, only the ACEO flow in the ethanol solution containing CH_3COONH_4 is stable and most intensive. It is considered that the solution flow is caused by ACEO when the applied AC voltage is less than 5.5 V. The flow rate is optimized with the solution conductivity 30.10μS/cm in the ac frequency range between 10 Hz and 50 Hz.

The electrochemical measurements show that electrochemical reaction can occur at lower voltage for ethanol solution containing these three electrolytes, and the main components participating in the electrochemical reaction are from the solution instead of the microelectrode

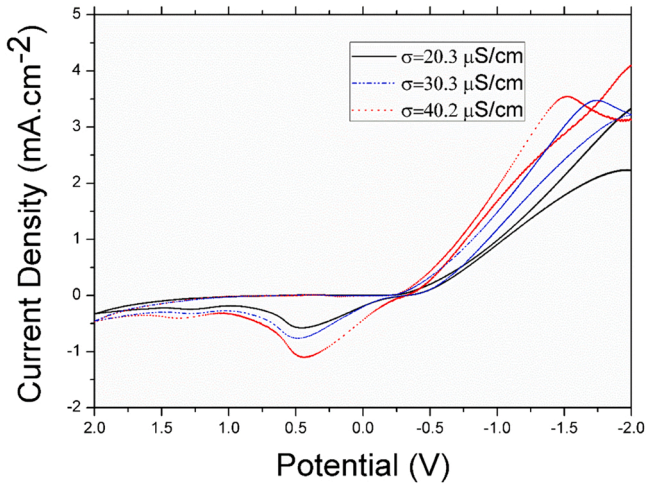

Fig. 12. Cyclic voltammograms of ethanol solution containing KOH on gold electrode. Scanning rate: 100 mV/s. Scanning from − 2–2 V, and sweeping back to − 2 V after reaching 2 V. Ag/AgCl.

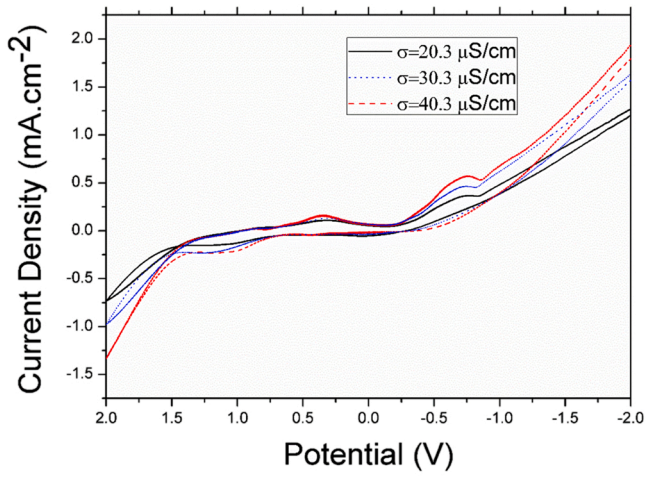

Fig. 13. Cyclic voltammograms of ethanol solution containing NH_4Cl on gold electrode. Scanning rate: 100 mV/s. Scanning from − 2–2 V, and sweeping back to − 2 V after reaching 2 V. Ag/AgCl.

dissipation. Among the three electrolytes, the REDOX currents in the ethanol solution containing KOH is the most intensive, while the REDOX currents in ethanol solution containing CH_3COONH_4 was the lowest. This may explain why the ethanol solution containing CH_3COONH_4 has a better ACEO flow using traveling-wave microelectrodes arrays. Compared with NH_4Cl and CH_3COONH_4 electrolytes, KOH is less prone to steric effect. This may explain why the ethanol solution with KOH has a better ACEO flow using the asymmetric microelectrode arrays. For the solution with NH_4Cl, both anodic and cathodic reactions produce gas. The gas produced by Faraday reaction may be responsible for the disordered flow in the ethanol solutions containing NH_4Cl in the traveling-wave ACEO experiments.

The results show that the ACEO drive of ethanol solution can be achieved by adding the optimized electrolyte and applying low voltage. The microelectrode arrays can be used in ethanol solution containing electrolyte for a long time, and no microelectrode damage was observed. This method shows better performance than EHD method. The current problem is that the mechanism of the influence of different electrolytes on ACEO is not fully understood. The main reason is that the electrochemical reaction of ethanol solution is very complicated, and the study of the electric double layer on the electrode surface is always difficult.

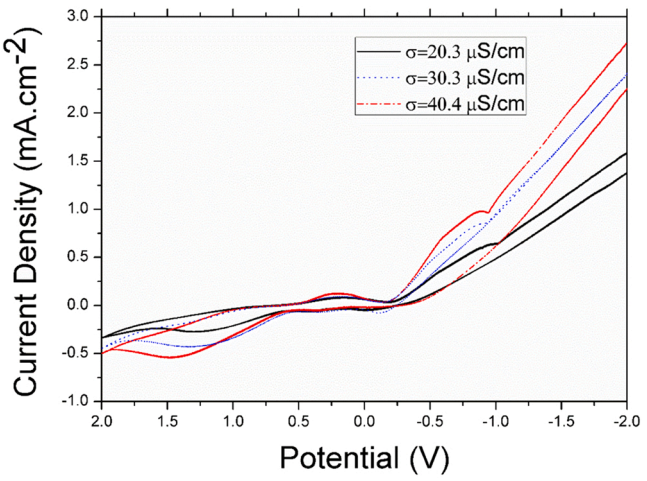

Fig. 14. Cyclic voltammograms of ethanol solution containing CH_3COONH_4 on gold electrode. Scanning rate: 100 mV/s. Scanning from − 2–2 V, and sweeping back to − 2 V after reaching 2 V. Ag/AgCl.

Therefore, this problem needs further study. Another problem is that both ethanol and water have strong electrochemical reactions. It is necessary to look for a new solution system that itself has a very weak electrochemical reaction, can dissolve the electrolyte, and can generate an ACEO drive by applying a low voltage. The solution system should be better used in microelectronic cooling systems. This aspect should be seriously considered in future work.

CRediT authorship contribution statement

Yong Yu: Conceptualization; Investigation; Resources; Writing – original draft; Project administration; **Ji-Cheng Li:** Data curation; **Hai Lin:** Visualization; **Kai Li:** Writing – review & editing; Supervision; Funding acquisition; **Fu-ting Yi:** Resources.

Declaration of Competing Interest

The authors declare that they have no known competing financial interests or personal relationships that could have appeared to influence the work reported in this paper.

Data availability

The authors do not have permission to share data.

Acknowledgement

This research is supported by the Strategic Pioneer Program on Space Science, Chinese Academy of Sciences (Grant No. XDA15012700), the National Nature Science Foundation of China (Grant No. 11972353), and the Key Research Program of Frontier Sciences, Chinese Academy of Sciences (Grant No. QYZDY-SSWJSC040).

References

[1] H.L. Lv, X.Y. Chen, X.Y. Li, Y.B. Ma, D.Y. Zhang, Finding the optimal design of a Cantor fractal-based AC electric micromixer with film heating sheet by a three-objective optimization approach, Int. Commun. Heat. Mass Transf. 131 (2022), 105867, https://doi.org/10.1016/j. icheatmasstransfer. 2021.105867.

[2] H.L. Lv, X.Y. Chen, New insights into the mechanism of fluid mixing in the micromixer based on alternating current electric heating with film heaters, Int. J. Heat. Mass Transf. 181 (2021), 121902, https://doi.org/10.1016/j. ijheatmasstransfer.2021.121902.

[3] H.L. Lv, X.Y. Chen, X.Y. Wang, X.W. Zeng, Y.B. Ma, A novel study on a micromixer with Cantor fractal obstacle through grey relational analysis, Int. J. Heat. Mass Transf. 183 (2022), 122159, https://doi.org/10.1016/j. ijheatmasstransfer.2021.122159.

[4] H.L. Lv, X.Y. Chen, X.W. Zeng, Optimization of micromixer with Cantor fractal baffle based on simulated annealing algorithm, Chaos Solitons Fractals 148 (2021), 111048, https://doi.org/10.1016/j.chaos.2021.111048.

[5] A. Manz, N. Graber, H.M. Widmer, Miniaturized total chemical analysis systems: a novel concept for chemical sensing, Sens. Actuators B Chem. 1 (1990) 244–248, https://doi.org/10.1016/0925-4005(90)80209-i.

[6] F. Hong, J. Cao, P. Cheng, Int. Commun. A parametric study of AC electrothermal flow in microchannels with asymmetrical interdigitated electrodes, Heat. Mass Transf. 38 (2011) 275–279, https://doi.org/10.1016/j. icheatmasstransfer.2010.11.004.

[7] V. Singhal, S.V. Garimella, A. Raman, Microscale pumping technologies for microchannel cooling systems, Appl. Mech. Rev. 57 (3) (2004) 191–221, https://doi.org/10.1115/1.1695401.

[8] B.D. Iverson, S.V. Garimella, Recent advances in microscale pumping technologies: a review and evaluation, Microfluid Nanofluidics 5 (2) (2008) 145–174, https://doi.org/10.1007/s10404-008-0266-8.

[9] N. Loucaides, A. Ramos, G. Georghiou, Novel systems for configurable AC electroosmotic pumping, Microfluid. Nanofluid. 3 (6) (2007) 709–714, https://doi.org/10.1007/s10404-007-0168-1.

[10] S.H. Ahn, Y.K. Kim, Fabrication and experiment of planar micro ion drag pump, Sens. Actuator A Phys. 70 (1–2) (1998) 1–5, https://doi.org/10.1016/s0924-4247(98)00105-8.

[11] C.C. Wong, D.R. Adkins, D. Chu, Development of a micropump for microelectronic cooling, 1996 Int. Mech. Eng. Congr. Exhibit. Atlanta, GA (1996) 1–6.

[12] S. Chowdhury, J. Darabi, M. Ohadi, J. Lawler, Chip integrated micro cooling system for high heat flux electronic cooling applications, 2002 Int. Conf. Thermal Challenges Next Generat. Electron. Syst. (2002) 85–93.

[13] V. Benetis, A. Shooshtari, P. Foroughi, M.M. Ohadi, 1 A sourceintegrated micropump for cooling of high heat flux electronics, 9th Annu. IEEE Semicond. Therm. Meas. Manag. Symp. (2003) 236–241.

[14] H. Yu, J. Yu, C. Ma, Design, fabrication and experimental research for an electrohydrodynamic micropump, Sci. China Technol. Sci. 53 (10) (2010) 2839–2845, https://doi.org/10.1007/s11431-010-4096-z.

[15] J. Darabi, M. Rada, M. Ohadi, J. Lawler, Design, fabrication, and testing of an electrohydrodynamic ion-drag micropump, J. Micro Syst. 11 (9) (2002) 684–690, https://doi.org/10.1109/jmems.2002.805046.

[16] S.F. Bart, L.S. Tavrow, M. Mehregany, J.H. Lang, Microfabricated electrohydrodynamic pumps, Sens. Actuators, Phys. A 21(1-3) ((1990) 193–197, https://doi.org/10.1016/0924-4247(90)85037-5.

[17] A. Richter, H. Sandmaier, An electrohydrodynamic pump, IEEE micro electro mechanical systems: an investigation of micro structures, Sens., Actuators, Mach. Robots (1990) 99–104, https://doi.org/10.1109/memsys.1990.110257.

[18] G. Fuhr, R. Hagedorn, T. Muller, W.J. Benecke, Microfabricated electrohydrodynamic (EHD) pumps for liquids of higher conductivity, Micro Syst. 1 (3) (1992) 141–146, https://doi.org/10.1109/84.186393.

[19] S.H. Ahn, Y.K. Kim, Fabrication and experiment of planar micro ion-drag pump, Sens. Actuators, Phys. A 70 (1–2) (1998) 1–5, https://doi.org/10.1016/s0924-4247(98)00105-8.

[20] J. Darabi, M.M. Ohadi, D. DeVoe, An electrohydrodynamic polarization micropump for electronic cooling, J. Micro Syst. 10 (1) (2001) 98–106, https://doi.org/10.1109/84.911097.

[21] I. Kano, K. Mizuochi, I. Takahashi, Micro-electrohydrodynamic pump by dielectric fluid: improvement for performance of pressure using cylindrical electrodes , Proceedings of the 6th JFPS International Symposium on Fluid Power, TSUKUBA, 2005 November 7–10 (2005) 575–579.

[22] I. Kano, I. Takahashi, Improvement for pressure performance of micro-EHD pump with an arrangement of thin cylindrical electrodes, JSME Int J. Ser. B 49 (3) (2006) 748–754, https://doi.org/10.1299/jsmeb.49.748.

[23] K. Aryana, A. Ghiami , M. Edalatpour, M. Passandideh-Fard, A review on Electrohydrodynamic (EHD) pumps, 24th Annual International Conference on Mechanical Engineering-ISME (2016) 1–6.

[24] O.M. Stuetzer, Ion drag pumps, J. Appl. Phys. 31 (1) (1960) 136–146, https://doi.org/10.1063/1.1735388.

[25] M. Siddiqui, J. Seyed-Yagoobi, Experimental study of liquid film pumping based on conduction phenomenon, IEEE Trans. Ind. Appl. 45 (1) (2009) 3–9, https://doi.org/10.1109/tia.2008.2009486.

[26] Y. Feng, J. Seyed-Yagoobi, Understanding of electrohydrodynamic conduction pumping phenomenon, Phys. Fluids 16 (7) (2004) 2432–2441, https://doi.org/10.1063/1.1739782.

[27] B.D. Iverson, S.V. Garimella, Experimental characterization of induction electrohydrodynamics for integrated microchannel pumping, J. Micromech. Microeng. 19 (5) (2009), 055015, https://doi.org/10.1088/0960-1317/19/5/055015.

[28] J. Seyed-Yagoobi, J.C. Qhato, J.M. Crowley, P.T. Krein, Induction electrahydradynamic pump in a vertical configuration: part 2—experimental study, J. Heat. Transf. 111 (3) (1989) 670–674, https://doi.org/10.1115/1.3250735.

[29] L.J. Yang, J.M. Wang, K.C. Ko, W.P. Shih, C.L. Dai, A circular microchannel integrated with embedded sprial electrodes used for fluid transportation, Sens. Actuator A Phys. 139 (1–2) (2007) 172–177, https://doi.org/10.1016/j.sna.2006.10.039.

[30] W.Y. Liu, Y.K. Ren, J.Y. Shao, H.Y. Jiang, Y.C. Ding, A theoretical and numerical investigation of travelling wave induction microfluidic pumping in a temperature

gradient, J. Phys. D: Appl. Phys. 47 (2014), 075501, https://doi.org/10.1088/0022-3727/47/7/075501.
[31] N. Islam, J. Reyna, Bi-directional flow induced by an AC electroosmotic micropump with DC voltage bias, Electrophoresis 33 (7) (2012) 1191–1197, https://doi.org/10.1002/elps.201100544.
[32] X.Y. Wang, C. Cheng, S. Wang, S.R. Liu, Electroosmotic pumps and their applications in microfluidic systems, Microfluid Nanofluid 6 (2) (2009) 145–162, https://doi.org/10.1007/s10404-008-0399-9.
[33] L. Li, X.Y. Wang, Q.S. Pu, S.R. Liu, Advancement of electroosmotic pump in microflow analysis: a review, Anal. Chim. Acta 1060 (2019) 1–16, https://doi.org/10.1016/j.aca.2019.02.004.
[34] A. Ramos, H. Morgan, N.G. Green, A. Castellanos, Ac electrokinetics: a review of forces in microelectrode structures, J. Phys. D. 31 (18) (1998) 2338–2353, https://doi.org/10.1088/0022-3727/31/18/021.
[35] A. Ramos, H. Morgan, N.G. Green, A. Castellanos, AC electric-field-induced fluid flow in microelectrodes, J. Colloid Interface Sci. 217 (2) (1999) 420–422, https://doi.org/10.1006/jcis.1999.6346.
[36] A. Ajdari, Pumping liquids using asymmetric electrode arrays, Phys. Rev. E 61 (1) (2000) R45–R48, https://doi.org/10.1103/physreve.61.r45.
[37] A. Brown, C. Smith, A. Rennie, Pumping of water with ac electric fields applied to asymmetric pairs of microelectrodes, Phys. Rev. E 63 (1) (2000), 016305, https://doi.org/10.1103/physreve.63.016305.
[38] A. Ramos, H. Morgan, N.G. Green, Pumping of liquids with traveling-wave electroosmosis, A. González, A. Castellanos, J. Appl. Phys. 97 (8) (2005), 084906, https://doi.org/10.1063/1.1873034.
[39] J. Hrdlicka, P. Cervenka, M. Pribyl, D. Snita, Mathematical modeling of AC electroosmosis in microfluidic and nanofluidic chips using equilibrium and non-equilibrium approaches, J. Appl. Electrochem. 40 (5) (2010) 967–980, https://doi.org/10.1007/s10800-009-9966-3.
[40] A. González, A. Ramos, P. García-Sánchez, A. Castellanos, Effect of the combined action of Faradaic currents and mobility differences in ac electro-osmosis, Phys. Rev. E 81 (1) (2010), 016320, https://doi.org/10.1103/physreve.81.016320.
[41] J. Wu, Ac electro-osmotic micropump by asymmetric electrode polarization, J. Appl. Phys. 103 (2) (2008), 024907, https://doi.org/10.1063/1.2832624.
[42] J.C. Li, K. Li, H. Lin, Y. Yu, Influences of the geometry of asymmetrical electrode arrays on the alternating current electro-osmosis flow in microchannels, Interfacial Phenom. Heat. Transf. 5 (2017) 1–8, https://doi.org/10.1615/InterfacPhenomHeatTransfer.2017021340.
[43] H. Sugioka, S. Segawa, Effective symmetry breaking of flow in AC electro-Osmotic pump using a ratchet structure, J. Phys. Soc. Jpn. 88 (2019), 084602, https://doi.org/10.7566/JPSJ.88.084602.
[44] K. Yoshida, T. Sato, S.I. Eom, J. Kim, S. Yokota, A study on an AC electroosmotic micropump using a square pole – slit electrode array, Sens. Actuator A Phys. 265 (2017) 152–160, https://doi.org/10.1016/j.sna.2017.08.026.
[45] M. Vazquez-Pinon, B. Pramanick, F.G. Ortega-Gama, V.H. Perez-Gonzalez, L. Kulinsky, M.J. Madou, H. Hwang, S.O. Martinez-Chapa, Hydrodynamic channeling as a controlled flow reversal mechanism for bidirectional AC electroosmotic pumping using glassy carbon microelectrode arrays, J. Micromech. Micro 29 (2019), 075007, https://doi.org/10.1088/1361-6439/ab1d9f.
[46] M. Vazquez-Pinon, B.C. Benítez, B. Pramanick, V.H. Perez-Gonzalez, M.J. Madou, S.O. Martinez-Chapa, H. Hwang, Direct current-induced breakdown to enhance reproducibility and performance of carbon-based interdigitated electrode arrays for AC electroosmotic micropumps, Sens. Actuator A Phys. 262 (2017) 10–17, https://doi.org/10.1016/j.sna.2017.05.023.
[47] J.P. Urbanski, T. Thorsen, J.A. Levitan, M.Z. Bazant, Fast ac electro-osmotic micropumps with nonplanar electrodes, Appl. Phys. Lett. 89 (2006), 143508, https://doi.org/10.1063/1.2358823.
[48] H.A. Rouabah, B.Y. Park, R.B. Zaouk, H. Morgan, M.J. Madou, N.G. Green, Design and fabrication of an ac-electro-osmosis micropump with 3D high-aspect-ratio electrodes using only SU-8, J. Micromech. Microeng. 21 (3) (2011), 035018, https://doi.org/10.1088/0960-1317/21/3/035018.
[49] Y.M. Senousy, C.K. Harnett, Fast three-dimensional ac electro-osmotic pumps with nonphotolithographic electrode patterning, Biomicrofluidics 4 (2010), 036501, https://doi.org/10.1063/1.3463719.
[50] X. Guo, K. Xie, 3D stepped electrodes on a flexible substrate with permanently bonded poly(dimethylsiloxane) channels for moving microfluid, J. Vac. Sci. Technol. B 31 (2013), 022002, https://doi.org/10.1116/1.4790651.
[51] B.P. Cahill, L.J. Heyderman, J. Gobrecht, A. Stemmer, Electro-osmotic streaming on application of traveling-wave electric fields, Phys. Rev. E 70 (2004), 036305, https://doi.org/10.1103/physreve.70.036305.
[52] B.P. Cahill, L.J. Heyderman, J. Gobrecht, A. Stemmer, Electro-osmotic pumping on application of phase-shifted signals to interdigitated electrodes, Sens. Actuators B Chem. 110 (2005) 157–163, https://doi.org/10.1016/j.snb.2005.01.006.
[53] M. Marczakand, H. Diesinger, Traveling wave dielectrophoresis micropump based on the dispersion of a capacitive electrode layer, J. Appl. Phys. 105 (2009), 124511, https://doi.org/10.1063/1.3152787.
[54] Y. Wu, Y. Ren, Y. Tao, H. Jiang, Fluid pumping and cells separation by DC-biased traveling wave electroosmosis and dielectrophoresis, Microfluid Nanofluid 21 (2017) 38, https://doi.org/10.1007/s10404-017-1862-2.
[55] N. Islam, D. Askari, Performance improvement of an AC electroosmotic micropump by hydrophobic surface modification, Microfluid Nanofluid 14 (2013) 627–635, https://doi.org/10.1007/s10404-012-1081-9.
[56] W.Y. Liu, Y.K. Ren, R. Xue, C.L. Song, Q.S. Wu, On ion transport regulation with field-effect nonlinear electroosmosis control in microfluidics embedding an ion-selective medium, Electrophoresis 41 (2020) 778–792, https://doi.org/10.1002/elps.201900408.
[57] W.Y. Liu, Y. Tao, R. Xue, C.L. Song, Q.S. Wu, Y.K. Ren, Continuous-flow nanoparticle trapping driven by hybrid electrokinetics in microfluidics, Electrophoresis 42 (2021) 939–949, https://doi.org/10.1002/elps.202000110.
[58] A. Dutta, J . Datta, Outstanding catalyst performance of PdAuNi nanoparticles for the anodic reaction in an alkaline direct ethanol (with anion-exchange membrane) fuel cell, J. Phys. C. Chem. 116 (2012) 25677–25688, https://doi.org/10.1021/jp305323s.
[59] C. Lamy, A. Lima, V. Lerhun, et al., Recent advances in the development of direct alcohol fuel cells (DAFC), J. Power Sources 105 (2) (2002) 283–296, https://doi.org/10.1016/s0378-7753(01)00954-5.
[60] K. Xie, Y. Lai, X. Guo, R.J. Campbell, A three phase serpentine micro electrode array for AC electroosmotic flow pumping, Micro Technol. 16 (10) (2010) 1825–1830, https://doi.org/10.1007/s00542-010-1106-9.
[61] S. Park, A. Beskok, Alternating current electrokinetic motion of colloidal particles on interdigitated microelectrodes, Anal. Chem. 80 (8) (2008) 2832–2841, https://doi.org/10.1021/ac7024859.
[62] B.D. Storey, L.R. Edwards, M.S. Kilic, M.Z. Bazant, Steric effects on ac electro-osmosis in dilute electrolytes, Phys. Rev. E 77 (2008), 036317, https://doi.org/10.1103/physreve.77.036317.
[63] G. Tremiliosi-Filho, E.R. Gonzalez, A.J. Motheo, E.M. Belgsir, J.M. Leger, C. Lamy, Electro-oxidation of ethanol on gold: analysis of the reaction products and mechanism, J. Electroanal. Chem. 444 (1998) 31–39, https://doi.org/10.1016/s0022-0728(97)00536-6.
[64] P. Garcıa-Sanchez, A. Ramos, Flow reversal in traveling-wave electrokinetics: an analysis of forces due to ionic concentration gradients, Langmuir 25 (9) (2009) 4988–4997, https://doi.org/10.1021/la803651e.
[65] M.S. Kilic, M.Z. Bazant, A. Ajdari, Steric effects in the dynamics of electrolytes at large applied voltages. I. Double-layer charging, Phys. Rev. E 75 (2007), 021502, https://doi.org/10.1103/PhysRevE.75.021502.
[66] P. Garcıa-Sanchez, A. Ramos, N.G. Green, H. Morgan, Traveling-wave electrokinetic micropumps: velocity, electrical current, and impedance measurements, Langmuir 24 (17) (2008) 9361–9369, https://doi.org/10.1021/la800423k.
[67] M.S. Arefin, T.L. Porter, An ac electroosmosis device for the detection of bioparticles with piezoresistive microcantilever sensors, J. Appl. Phys. 111 (5) (2012), 054919, https://doi.org/10.1063/1.3693538.
[68] P. Garcıa-Sanchez, A. Ramos, A. González, Effects of faradaic currents on AC electroosmotic flows with coplanar symmetric electrodes, Colloids Surf. A Physicochem. Eng. Asp. 376 (1–3) (2011) 47–52, https://doi.org/10.1016/j.colsurfa.2010.11.006.

Yong Yu: Associate Professor , CAS Key Laboratory of Microgravity,Institute of Mechanics, Chinese Academy of Sciences. In 1997, I received the Master's degree in analytical Chemistry from Shandong University, China. In 2000, I received PhD in physical chemistry from the department of chemistry, Beijing Normal University. From August 2000 to September 2002, I worked as a postdoctoral fellow in the Institute of Mechanics, Chinese Academy of Sciences, and then worked in the Institute. From November 2008 to May 2009, I was a visiting scholar in the research group of Professor Betzel, Department of Biochemistry and Molecular Biology, University of Hamburg, Germany. The main research interests are proteins crystallization mechanism in space and drive technology of alternating current electroosmosis.